Monitoring the 1992 Forest Fires in the Boreal Ecosystem Using NOAA AVHRR Satellite Imagery

Donald R. Cahoon, Jr., Brian J. Stocks, Joel S. Levine, Wesley R. Cofer III, and James A. Barber

The boreal ecosystem is a forested belt, mostly comprising conifer trees, which stretches across the Northern Hemisphere's circumpolar countries. The boreal forest covers more than 12 million km^2 of the earth's surface, or about 10% of the land surface. In areal extent, the boreal forest ranks about fifth among terrestrial biomes, but ranks second only to tropical forests in total plant mass (Whittaker and Likens 1975). Given the ecosystem's size and total available plant mass it is understandable that the world's boreal forests contain almost 40% of terrestrial carbon (Kasischke et al. 1995). The boreal forest must therefore play an extremely important role in the global carbon budget and it is vital to identify anything that perturbs the carbon cycle within this ecosystem. Fire is one such disturbance.

An important factor in the composition and evolution of the boreal forest is fire. Fire is predominantly a natural phenomenon, but with increasing population pressures the incidence of human-initiated fires is increasing. The boreal fire-return interval is estimated to range from 50 to 240 years, and it is known that the interannual fire disturbance throughout the boreal system can vary widely. But there is little in the way of hard numbers to quantify that interannual variance. This uncertainty particularly applies in Russia, which takes in about two thirds of the boreal ecosystem. Much of the uncertainty about the annual areal extent of boreal forest fires is a result of the remoteness of this ecosystem. Even though it is typical for fire outbreaks to occur over hundreds of kilometers in range, this ecosystem is so vast and its population is so sparse in many areas that these fires are difficult to closely monitor. Another important aspect of boreal fires is that relatively few large fires can burn unnoticed for weeks and yet account for the vast majority of the area burned in any given season. It is estimated that about 95% of the total area is burned by 5% of the fires. The very nature of fire in the boreal system with geographically widespread and spatially large outbreaks, combined with the remote ecosystem, makes satellite remote sensing an important tool in monitoring boreal forest fires.

For the year 1992, we collected and processed 1-km (nadir) AVHRR (Advanced Very High Resolution Radiometer) satellite imagery to estimate the area burned in Russia. Using the AVHRR-derived area-burned estimate and other factors derived from previous field campaigns in the boreal forest, we estimated the atmospheric loading of carbon dioxide (CO_2), carbon monoxide (CO), and methane (CH_4). The methodology employed in this study follows that of a similar analysis for the year 1987 (Cahoon et al. 1994).

AVHRR Processing

More than 7 gigabytes of 1-km (nadir) imagery have been acquired to monitor the Russian 1992 seasonal fire progression and to provide an estimate of the total forested area burned. Given the large volume of AVHRR imagery acquired and the large geographical range studied, the analysis, which extended from 30 to 180°E longitude and 45 to 75°N latitude, was broken up into $30 \times 30°$ geographical boxes (figure 75.1). Each individual AVHRR image was processed from the NOAA level 1b Local Area Coverage (LAC) formatted archival product (Kidwell 1991). The level 1b imagery was first calibrated to convert instrument digital counts to radiance (Rao 1993; Rao and Chen 1994). Instrument degradation was also corrected for when converting from digital signals to radiance. Other corrections to the radiance were made to properly adjust for varying solar and spacecraft geometry. The calibrated radiance was further reduced to surface reflectance (AVHRR channels 1 and 2) and to temperature (AVHRR channels 3, 4, and 5). Each of the individual scenes was then navigated and geographically mapped into one of the five defined geographical boxes.

Following the procedure detailed in Cahoon et al. (1994), a composite for each of the five geographical boxes was created from all the individual scenes that fit

Monitoring the 1992 forest fires in the boreal ecosystem using NOAA AVHRR satellite imagery. 1993. Cahoon, D.R.; Stocks, B.J.; Levine, J.S.; Cofer, W.R.; Barber, J.A. Pages 795-801 (Vol. 2, Chapter 75) in J.S. Levine, editor. Biomass Burning and Global Change. NASA, Florida, USA.

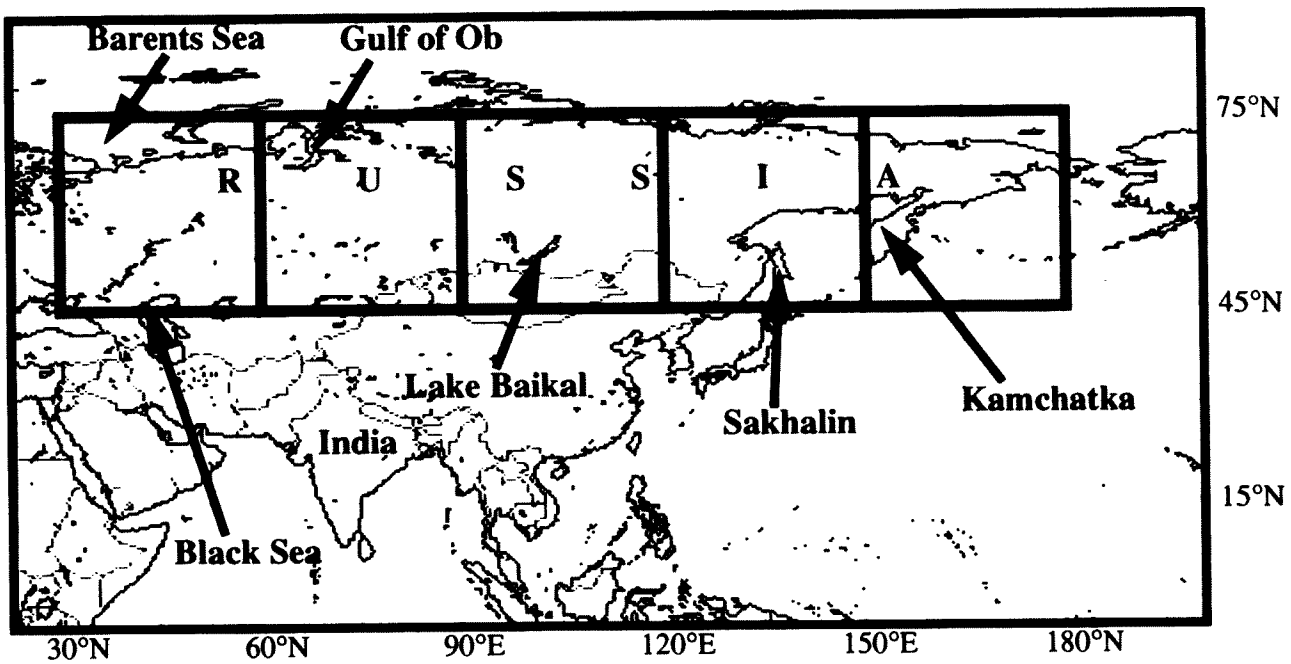

Figure 75.1 Each of the fire geographical regions processed separately is outlined by the bold-lined boxes that cover most of Russia.

within each box. The composites were used to identify regions of data gaps, whether from missing satellite coverage or cloud cover, and were critical for quickly assessing the geographical regions that required additional imagery to provide adequate clear-sky coverage. In addition to providing information about usable satellite clear-sky data coverage, each individually mapped scene was examined for indications of active forest fires. This information was the basis for establishing the time-history of fire outbreaks, which was used for validating burn scars identified in later processing. The geographically mapped composite scenes were also used to optimize selection of individual images for the final area estimation. This selection procedure enabled the highest-quality images to be used in estimating the burned area and to ensure that no overlapping burned areas lay between any of the individual scenes being processed.

Methods—Estimating Burned Area

A multispectral minimum-distance classification approach identifies and segments the pixels that include burned areas. Identifying burned area depends upon the unique spectral characteristics, in both the shortwave and longwave part of the spectrum, of the burned scars that can be contrasted with the spectral characteristics of other surfaces. Surface reflectivity in the near-infrared drops significantly after the forest has been burned (Bowker et al. 1985). This drop in surface reflectance provides a clear physical signal of vegetation damage, but other spectral bands are needed to further differentiate the fire scars from other surfaces. In particular, water has a reflectance similar to that of burned area in the near-infrared. The combination of visible and thermal AVHRR channels is required to distinguish water from fire scars as well as to distinguish other features, such as smoke and clouds (Cahoon et al. 1994; Chung and Le 1984). The segmented, burned scar pixels are saved as an image for each of the five geographical regions and are subjected to the surface-area estimation algorithm.

The burned pixel maps are processed for surface-area estimation following the methodologies that have been developed in Cahoon et al. (1992, 1994). The surface area of the geographically mapped fire-scar pixels in each of the burned-area maps is geometrically computed. The surface area of the fire-scar pixel is a function of latitude, longitude, and the geographical projections into which the images are mapped. The surface area is estimated using AVHRR 1-km data for 25 targets of known size and an AHVRR measurement error is determined for each target. The documented target sizes (Environment Canada 1973) have an error associated with their reported measurements. The error of both the AVHRR estimate and the

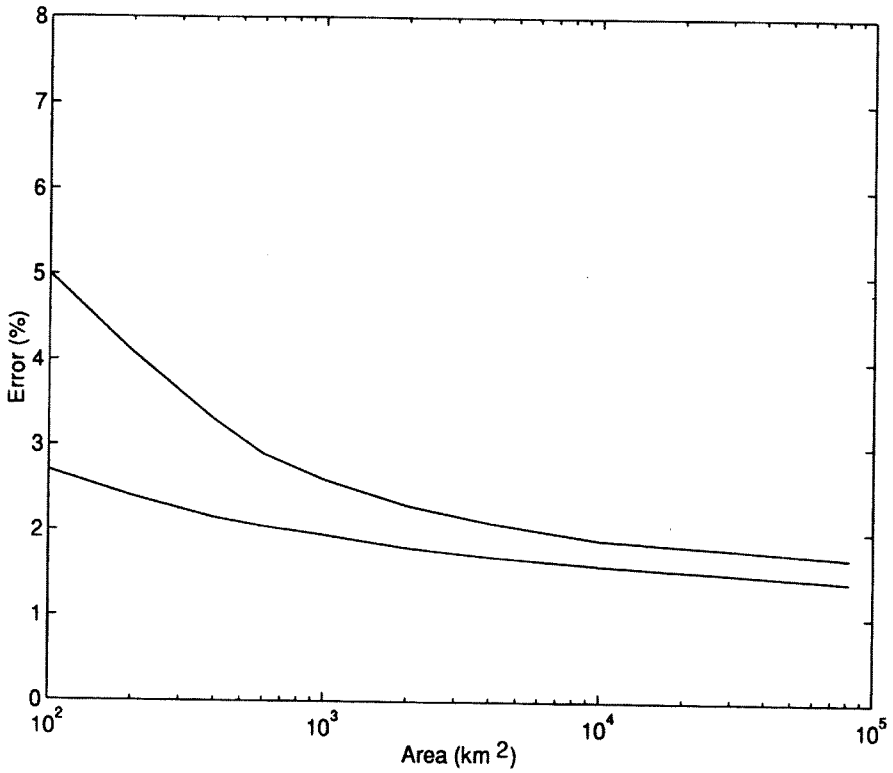

Figure 75.2 The AVHRR 1-km surface area estimate errors are plotted as a function of the target size. The lower curve is the mean error. The upper curve contains 95% of all of the surface area estimate errors and never exceeds 5%. These two curves show how the error and the overall uncertainty decreases with an increasing target size.

documented target size is low for larger targets and increasingly higher for targets that are smaller than 1000 km^2.

The documented errors in target size are broken down into a mean error and an upper-bound error that encompass 90% of observations. The same is done for the AVHRR error estimates by fitting curves through the mean and second standard deviation values that result from computing all error estimates in a sliding window, which is a function of target size. The purpose of the sliding window is to reasonably represent the increasing error variance about the mean with decreasing target size. The AVHRR error estimate curves mirrored those of the documented target sizes (but were higher) indicating that some of the uncertainty in the AVHRR error estimates can be clearly attributed to uncertainty in the reported target size. The uncertainty in the documented target sizes is removed from the AVHRR error estimates, and figure 75.2 shows the resulting curves. The 1-km AVHRR error estimate curves show that 95% of the AVHRR estimates fall within a 5% error range for a target size of 100 km^2 and for the mean curve the error is 3.5%. Both curves level out in the range below 2% error once the target size exceeds about 1000 km^2. The AVHRR area estimates used in this study are reported using the conservative range of 5%, when in fact, given the size and total contribution of area burned in large boreal forest fires, the actual error in the estimate is likely to be a few percent smaller.

Very much of the uncertainty in the surface-area estimates results from overlapping observations of the ground. This overlap, which can be attributed to both spacecraft earth geometry and the instrument itself, has the effect of blurring the image acquired. To estimate the size of any area, it is imperative to concisely realize the spatial region's outer boundary. Boundaries of any region in an AVHRR image are not crisp by any means, because each footprint (one pixel in the image) on the ground overlaps adjacent footprints and a boundary can be shared between pixels. It can easily take several pixels to totally escape the effects of a point on the surface, even though, in a purely geometric sense (using the instantaneous field of view [IFOV]), that location may be observed in only one footprint. This inability to record a unique piece of ground without remembering prior observations leaves the resulting pixel value a weighting of values to either side of the distinct boundary (e.g., unburned and burned forest, land and water). The image-processing methods discussed in the earlier section are used to decide how to separate boundary pixels that mix both

scene types. This decision is accomplished by statistically determining the spectral characteristics in the two adjoining scene types and then determining the mathematical point of separation so that pixels with mixed scene types can be classified as a particular scene type. This procedure is crucial to ensure that the burned areas are arrived at objectively, repeatedly, and reliably.

Methods—Gaseous Emissions Estimates

The satellite-derived burned-area estimates are used to compute the total forest-fire combustion emissions of CO_2, CO, and CH_4 to the atmosphere. The methodology followed is similar to that of Seiler and Crutzen (1980), but is modified to incorporate boreal-forest specific data that are acquired by more recent field-research campaigns (Alexander et al. 1991; Cofer et al. 1990; Stocks 1987, 1989). Data from prior and continuing research (Cofer et al., this volume; FIRESCAN Team papers, this volume) are invaluable in modeling the emissions. The uncertainty of CO_2 normalized emission ratios is not clearly defined, but given the more recent work by Cofer et al. (this volume), the values that are used for computing the total emissions are considered conservative. The same is true for the average fuel consumption, in which Kasischke et al. (1995) have determined values that are slightly higher than those used in this study. Although the uncertainties are being addressed in research, decidedly conservative values are used in estimating the emissions, with the expected result of estimating lower than actual atmospheric emissions.

The emission calculations are based on the equation:

$$E_x = F \times 0.45 \times A \times S_{FS} \times ER_{FS} \times \frac{X_{mw}}{12},$$

where E_x is the total emission of gas specie x, F is the fuel consumed (2.5 kg m^{-2}), 0.45 is the fractional mass of C in the fuel consumed, A is the total area burned, S_{FS} is the fractional time spent in either flaming or smoldering combustion stage; ER_{FS} is emission ratio for gas x in either flaming and smoldering combustion stage, and $X_{mn}/12$ relates the kg of gas x to kg C. The emission ratios are presented in table 75.1. For this analysis, it is assumed that the time spent in either flaming or smoldering combustion stages is 50% (we have few supporting data for this assumption). It is important to realize that if 80% of the C is consumed in either combustion stage, the emissions will vary by 2%, 18%, and 21% for CO_2, CO, and CH_4, respectively.

Table 75.1 Mean emission ratios for two combustion stages in the boreal forest. The remaining C is released in particulate form.

	Mean emission ratio (%)	
Combustion stage	CO	CH_4
Flaming	6.60	0.61
Smoldering	12.30	1.26

1992 Fire Season

Widespread forest fires occurred in several regions of Russia in 1992. These regions are identified in figure 75.3. Even though there are a number of widespread fire outbreaks, fire growth is likely to be limited by meteorological conditions not favorable for sustained fire development. In 1992, the total AVHRR estimate for burned area in Russia was 1 496 727 ha. Figure 75.3 shows the distribution of burned area relative to each of the five geographic regions. The region from 60 to 90°E longitude has no discernible burn scars. Even with some of the obvious data gaps shown in figure 75.3, the majority of the boreal ecosystem has sufficient clear-sky satellite coverage. The regions with most burn scars are to the east, where clear-sky coverage is best. The reason for higher burned areas to the east is likely to be the increase in population to the west and the low marshy areas west of the Yenisey River. With the population increase to the west come additional fire-management pressures and better access to fires for suppression purposes.

In eastern Russia the population density averages less than one inhabitant km^2, permitting reduced fire-management concerns. Also, reduced population requires less infrastructure to support aggressive fire suppression. Many of these regions are so vast and isolated that monitoring fire activity by aircraft is difficult and expensive. Thus, 1992 was typical in that the largest amount of forest burned was east of the Yenisey River (running approximately north and south along 90°E longitude). The marshy region west of the Yenisey River also helps limit fire growth by isolating tracts of forest and minimizing the total area burned. The 1992 fire season was also typical in terms of the interannual fire variability. Figure 75.4 shows the variability for two decades of burned-area records compiled by Dixon et al. (1993). The AVHRR-derived burned-area estimates for 1987 (Cahoon et al. 1994) and 1992 are included in figure 75.4 and further show evidence of the potential for large interannual swings in the total area burned. In 1987, the area burned was 14.5 million ha, which is more than an order of magnitude greater than that in 1992.

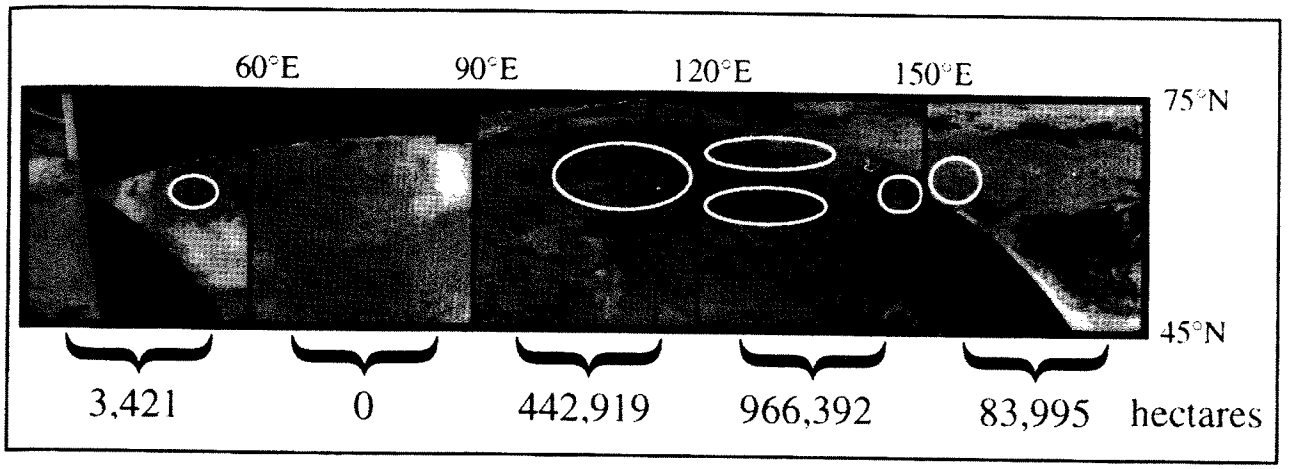

Figure 75.3 Composite of all of the available 1992 AVHRR 1-km coverage that is used in creating a mostly clear-sky scene. Dark gray is water, light gray is land and clouds, and black regions denote areas where clear-sky coverage is not available. The five geographical regions are superimposed. The circles enclose areas that experienced widespread fire activity. The area burned in each of the five regions is reported in hectares.

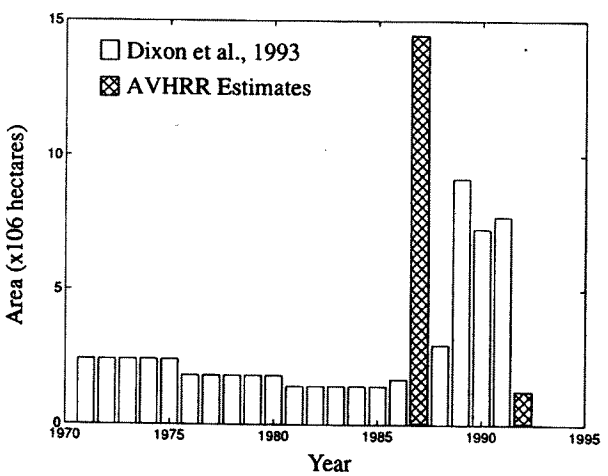

Figure 75.4 Histogram showing the current state-of-knowledge of the interannual variability of the total area burned in Russia. Dixon et al. (1993)-reported values are the solid white bars and the AVHRR-derived estimates are in hatched columns.

In 1992 the total area burned across both Alaska (51 779 ha) and Canada (841 201 ha) was also low (Personal communication with David Hendren, Alaska Interagency Fire Coordination Center; Canadian Committee on Forest Fire Management, 1992). This figure brings the total area burned for the entire boreal ecosystem (assuming minimal fire extent in Scandinavia) to about 2.4 million ha, a relatively quiet year compared to a year such as 1987 with more extreme fire activity. Based on these burned-area estimates, fire emissions are estimated for Russia and for the entire boreal ecosystem, and are compared to the estimated annual emissions for African savannas (Lacaux et al. 1993) and the estimated total global emissions from biomass burning (Andreae 1991) table 75.2. We draw the comparison with the African savannas because this is a large ecosystem that experiences spatially extensive burning annually. It is interesting that the boreal ecosystem contributes more of the reduced carbon species relative to that of CO_2 compared to the African savannas since there is more incomplete combustion in the high-intensity boreal forest fires than in African savanna fires.

Discussion

AVHRR 1-km satellite imagery is used to monitor Russian forest-fire activity in the boreal ecosystem. This research follows the methods detailed in Cahoon et al. (1992, 1994). Clear-sky coverage is obtained for the Russian boreal forest and the surface area burned is estimated. In 1992, the total area burned in Russia is about 1.5 million ha. This value is considerably lower than the AVHRR estimate for 1987, which is 14.5 million ha. The gaseous emissions are estimated for the Russian fires based on the surface-area burned estimates and ecosystem-dependent measurements acquired in field studies. The overall emissions are lower than those in 1987 by an order of magnitude, and both years are compared to the estimated emissions from African savannas, where fire reaches the greatest spatial extent on any continent, and the estimated annual global emissions from biomass burning. The annual emissions from boreal forest fires is a

Table 75.2 Emission comparisons (g element)

	CO_2	CO	CH_4
1992 Russian forest fires	1.47×10^{13}	1.59×10^{12}	1.57×10^{11}
1992 Boreal-wide forest fires	2.36×10^{13}	2.55×10^{12}	2.52×10^{11}
1987 East Asian fires	1.42×10^{14}	1.54×10^{13}	1.52×10^{12}
Savanna fire emissions/yr	7.00×10^{14}	4.25×10^{13}	2.20×10^{12}
Global biomass burning emissions/yr	3.50×10^{15}	3.50×10^{14}	3.80×10^{13}
Ratio of 1987 East Asian/1992 boreal-wide fire emissions to savanna fire emissions (%)	20/3	36/6	69/11
Contribution of 1987 East Asian/1992 boreal-wide fire emissions to global emissions (%)	4/1	4/1	4/1

significant fraction of the total biomass burning emissions during years of intense activity. Of course, if the tropical emissions have been overestimated, the relative contribution of boreal forest fires will increase accordingly.

The 1992 fire season in Russia, Alaska, and Canada was not dramatic by any means. However, even though this was a year of relatively minimal burning overall, it exemplifies characteristics that are typical of fire in the boreal ecosystem. Fires in that ecosystem exhibit a large interannual variation in area burned and variable geographic distribution. Also, it has been shown that there is more Russian fire activity east of the Yenisey River due to orographic and population considerations. The increase in fires toward the east, along with all its variabilities, demonstrates the significance of the natural forces in action, which shape the composition and evolution of the boreal forest, largely without human intervention. For long-term research investigations whose foci are the natural evolutionary changes in the boreal forest and drivers of this change, the region east of the Yenisey River should be of primary interest.

The total area burned in boreal forest can vary by more than one order of magnitude. This variability contrasts starkly to what is believed to occur in the African savanna ecosystem, where the geographic range and distribution of fires appear to be very similar from year to year (Cahoon et al. 1992). The reason for such contrast is that human population pressures are the primary source of fire activity in the savannas, and in the boreal system the fires are predominantly natural. This source highlights the importance of meteorological conditions (e.g., temperature, humidity, winds, precipitation, and lightning) in shaping fire activity in the boreal ecosystem. Further, with meteorology so crucial, it can be assumed that climatic variations must have a dominant role in modifying the composition and evolution of the boreal ecosystem. Given that upward of 40% of terrestrial carbon is stored in this ecosystem and that fire releases large amounts of carbon to the atmosphere, carbon cycling between the boreal forest and the atmosphere would be likely to be significant in global climatic change.

Acknowledgments

The research in this chapter is supported by the Environmental Protection Agency through interagency agreements (DW80936130-01-0 and DW80936541-01-0) with the National Aeronautics and Space Administration.

References

Alexander, M. E., B. J. Stocks, and B. D. Lawson. (1991). Predicting fire behavior in the black spruce-lichen woodland: The Porter Lake Project, Report prepared for Canadian Northern Forest Centre, Edmonton, AB, Report no. NOR-X-310.

Andreae, M. O. 1991. Biomass burning: Its history, use, and distribution and its impact on environmental quality and global change. In *Global Biomass Burning: Atmospheric, Climatic, and Biospheric Implications*, MIT Press, Cambridge Mass., 3–21.

Bowker, D. E., R. E. Davis, D. L. Myrick, K. Stacy, and W. T. Jones. 1985. Spectral Reflectances of Natural Targets for use in Remote Sensing Studies, NASA Reference Publication 1139, Hampton, Va.

Cahoon, D. R., Jr., B. J. Stocks, J. S. Levine, W. R. Cofer III, and C. C. Chung. 1992. Evaluation of a technique for satellite-derived estimation of biomass burning. *J. Geophys. Res.*, 97(D4), 3805–3814.

Cahoon, D. R., Jr., B. J. Stocks, J. S. Levine, W. R. Cofer III, and J. M. Pierson. 1994. Satellite analysis of the severe 1987 forest fires in northern China and southeastern Siberia. *J. Geophys. Res.*, 99(D9), 18 627–18 638.

Canadian Committee on Forest Fire Management. 1992. Reports Tabulated at Forty-First Annual Meeting, Winnipeg, Manitoba, November 19–20.

Chung, Y. S., and H. V. Le. 1984. Detection of forest-fire smoke plumes by satellite imagery. *Atmos. Environ.*, 18(10), 2143–2151.

Cofer, W. R., III, J. S. Levine, E. L. Winstead, and B. J. Stocks. 1990. Gaseous emissions from Canadian boreal forest fires. *Atmos. Environ.*, 24A, 1653–1659.

Dixon, R. K., and O. N. Krankina. 1993. Forest fires in Russia: Carbon dioxide emissions to the atmosphere. *Can. J. For. Res.*, 23, 700–705.

Environment Canada/Inland Waters Directorate/Water Resources Branch. 1973. Inventory of Canadian freshwater lakes, Ottawa, Canada.

Kasischke, E. S., N. H. F. French, L. L. Bourgeau-Chavez, N. L. Christensen, Jr. 1995. Estimating release of carbon from 1990 and 1991 forest fires in Alaska. *J. Geophys. Res.*, 100, 2941–2951.

Kidwell, K. B. 1991. NOAA Polar Orbiter Data (TIROS-N, NOAA-6, NOAA-7, NOAA-8, NOAA-9, NOAA-10, NOAA-11) Users Guide. National Environmental Satellite Data and Information Service, Washington, D.C.

Lacaux, J. P., H. Cachier, and R. Delmas. 1993. Biomass burning in Africa: An overview of its impact on atmospheric chemistry. In *Fire in the Environment: The Ecological, Atmospheric, and Climatic Importance of Vegetation Fires*, John Wiley, New York, 159–191.

Rao, C. R. N., J. T. Sullivan, C. C. Walton, J. W. Brown, and R. H. Evans. 1993. Nonlinearity corrections for the thermal infrared channels of the Advanced Very High Resolution Radiometer: Assessment and recommendations. NOAA Technical Report NESDIS 69, Washington, D.C.

Rao, C. R. N., and J. Chen. 1994. Post-launch calibration of the visible and near infrared channels of the Advanced Very High Resolution Radiometer on NOAA-7, -9, and -11 spacecraft. NOAA Technical Report NESDIS 78, Washington, D.C.

Seiler, W., and P. J. Crutzen. 1980. Estimates of gross and net fluxes of carbon between the biosphere and the atmosphere from biomass burning. *Climatic Change*, 2, 407–247.

Stocks, B. J. 1987. Fire behavior in immature jack pine. *Can. J. For. Res.*, 17, 80–86.

Stocks, B. J. 1989. Fire behavior in mature jack pine. *Can. J. For. Res.*, 19, 783–790.

Stocks, B. J. 1991. The extent and impact of forest fires in northern circumpolar countries. In *Global Biomass Burning: Atmospheric, Climatic, and Biospheric Implications*, MIT Press, Cambridge, Mass., pp. 197–202.

U.S. Department of the Interior/Bureau of Land Management 1992. 1992 Alaska Fire Service Fire Season Statistics.

Whittaker, R. H., and G. E. Likens. 1975. Primary production: The biosphere and man. In *Primary Productivity of the Biosphere*, Ecological Studies 14, H. Leith and R. H. Whittaker, eds., Springer-Verlag, New York.